Numerical investigation of the role of non-uniform evaporation rate in initiating Marangoni convection in capillary tubes

Received March 2003
Revised October 2003
Accepted December 2003

R. Bennacer
LEEVAM-LEEE, Université de Cergy Pontoise, Neuville sur Oise, France
K. Sefiane
School of Chemical Engineering, University of Edinburgh, Edinburgh, UK
M. El-Ganaoui
Faculté des Sciences et Techniques, Université de Limoges, Limoges, France
C. Buffone
School of Chemical Engineering, University of Edinburgh, Edinburgh, UK

Keywords *Convection, Flow, Liquids, Channel flow, Evaporation*

Abstract *A computational model is developed to describe convection in volatile liquids evaporating in capillary tubes. Experimental work has demonstrated the existence of such convective structures. The correlation between this convection and the phase change process has been experimentally established. Temperature distribution on the liquid-vapour interface is considered in order to characterise the minimum of radial temperature gradient required to initiate and orientate Marangoni convection. Direct numerical simulation using finite volume approximation is used to investigate the heat and mass transfer in the liquid phase. The case of a capillary tube filled with a volatile liquid is investigated for various Marangoni numbers, to characterise heat and mass transfers under conditions close to realistic operating parameters. The simulation shows that a minimum irregularity in evaporative flux along the liquid-vapour interface is necessary to trigger thermocapillary convection. The enhancement of heat and mass transfer by Marangoni convection is also investigated.*

Nomenclature

A = annulus aspect ratio ($A = L/R$)
L = height of the domain (m)
Ma = Marangoni number ($= -(\partial\sigma/\partial T)\,\Delta T\,R/\mu\alpha$)
Pr = Prandtl number ($= \nu/\alpha$)
Q = dimensional applied flux (W/m^2)
q = dimensionless applied flux
r, z = dimensionless coordinate in the radial, axial direction,
R = radius of the considered domain (m)
T = dimensionless temperature ($= (T' - T_0)/\Delta T$)
ΔT = reference temperature difference ($= Q_0 R/\lambda$)(K)
u_r, u_z = dimensionless velocity in r, z direction ($u'_r R/\alpha$, $u'_z R/\alpha$)

Greek symbols

α = thermal diffusivity (m^2/s)
γ = rate change tension surface vs temperature ($\gamma = \partial\sigma/\partial T$)
λ = thermal conductivity (W/m^{2}K)
Ψ = dimensionless stream function ($\Psi'/\alpha R$)

International Journal of Numerical Methods for Heat & Fluid Flow
Vol. 14 No. 7, 2004
pp. 879-892

0961-5539
DOI 10.1108/09615530410546281

μ = dynamic viscosity (kg/m s)
ν = kinematic viscosity (m^2/s)
ρ = density (kg/m^3)
ρC = heat capacity ($J/K\,m^3$)
σ = surface tension (N/m)

Subscripts
0 = reference
max, min = maximum, minimum

Introduction

Many technological applications involve evaporation of liquids in confined environment. The behaviour of wetting menisci accompanied with phase change has been the subject of extensive studies during the last decades (Morris, 2001). This is a very important issue in the design of cooling devices like micro-heat pipes; due to the effects it will have on heat transfer capacity. In addition, given the magnitude of the local evaporative heat fluxes from the meniscus in these cases there is great potential for their use as cooling techniques in high power systems. Much work has been carried out to try to model the evaporation process and predict how the meniscus is affected by different parameters. Wayner and Potash (Morris, 2001) investigated the transport processes that occurred in a two-dimensional evaporating meniscus and adsorbed thin film on a superheated flat glass plate immersed in a liquid. They concluded that a change in the profile of the meniscus brings about a pressure drop that is sufficient to give the fluid flow required for evaporation, i.e. it circulates fluid so that it replaces the liquid that has evaporated and hence allows the evaporation to continue. It was also shown that in the intrinsic meniscus region fluid flow is brought about by thermocapillarity while in the evaporating thin film region the fluid flow is entirely caused by the disjoining pressure gradient between the film and the vapour. The convection currents formed in the liquid just below the meniscus could increase the heat transfer coefficient by up to 30 per cent (Khrustalev and Faghri, 1994). This is presumably due to the assistance of the convection current in bringing liquid from the bulk region right up to the interface where the heat transfer occurs, and then removing it again. Furthermore, Molenkamp (1998) demonstrated that in containers with a diameter greater than a few millimetres, convection motion is dominated by natural convection (buoyancy). In capillary tubes with a diameter less than a critical value we can expect that there will be convection rolls due to thermocapillarity, instead of Rayleigh convection. During evaporation different characteristic regions of the meniscus are formed by the liquid, such regions are identified by Holm and Golpen (1979) during evaporation from a grooved plate. The surface tension variations result from a non-uniform temperature, and drive the flow of the fluid inducing thermocapillary (or Marangoni) convection. The Marangoni number ratio of the acting surface tension forces to the viscous forces is used as a control parameter for such configurations. The challenge remains how to access to local surface tension via the local temperature; it is of paramount importance to understand the phenomenon. In recent work, (Höhmann and Stephan, 2002), have investigated the temperature profile underneath an evaporating meniscus using thermographic liquid crystals (TLC) with a sub-micron spatial resolution. It is demonstrated that the temperature profile exhibits a minimum near the contact line where evaporation is largest. The temperature decrease is thought to be caused by the evaporative cooling effect. Kim and Wayner (1996) have investigated the evaporative mass flux profile as well as the meniscus thickness for volatile liquids. They have developed a model relating evaporating mass flux to the

meniscus thickness in the macro-region. It has been shown that the evaporation profile presents a maximum near the contact line. (Sefiane and Steinchen, 2002) conducted experiments on evaporation of volatile liquids in capillaries showing strong convection rolls clearly related to evaporation. This convection has been characterised in various configurations and fluids. Figure 1(a) shows an image of the thermocapillary convection observed in the evaporating meniscus and the global flow pattern (streamtraces) that can be obtained by image processing of succesive images as represented on Figure 1(b). In the experiments, a steady contact angle was investigated where evaporation takes place in dry air and liquid is supplied to compensate the evaporation.

A key question is: considering a non-uniform evaporation, what is the minimum irregularity in the evaporation rate along the liquid-vapour interface, which would trigger thermocapillary convection? As it is difficult to address this issue experimentally, a numerical approach is adopted in a simplified 2D geometry close to the experimental parameters. The aim of this paper is to simulate the effect of various evaporation profiles along the meniscus. By solving numerically the full model with appropriate boundary conditions, the velocity field in the bulk liquid is described for the different considered heat flux profiles. Conditions under which convection appear and develop are analysed. The results are compared with available experimental observations.

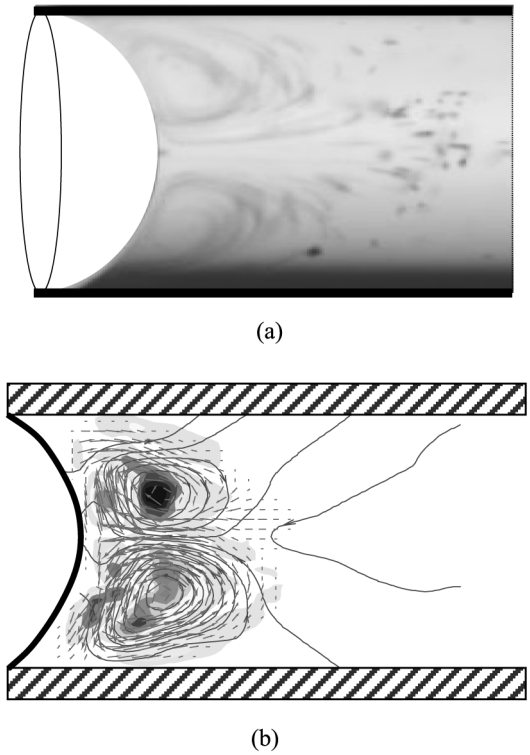

Figure 1.
Experimental result showing thermocapillary convection rolls (Sefiane and Steinchen, 2002), instantaneous image (a) and image processing using PIV technique showing the streamlines (b)

Problem modelling

It is established experimentally that thermocapillary convection related to interfacial conditions takes place when volatile liquids evaporate in capillary tubes Sefiane and Steinchen (2002). In the following, the analysis of the controlling parameters is performed. Indeed, interfacial conditions are dictated by the various heat and mass fluxes operating during the process. Such typical coupled problem, drawn in Figure 2, involves heat conduction in the liquid phase towards the interface and inside the solid wall. Conduction in the vapour phase could be neglected because of the weak thermal conductivity. At the liquid-vapour interface, the heat flux corresponding to the phase change must satisfy both the energy and the species conservation. The generated vapour is transported from the interface to the bulk gas by diffusion. Because the meniscus wedge is near the solid wall and the cylindrical configuration, a larger heat flux is transferred to the closer fluid than to the centre resulting in a higher evaporation rate near the contact line. This non-uniform evaporation rate induces a non-uniform temperature distribution on the interface. Since surface tension for most liquids is a decreasing function of the temperature, a surface tension gradient along the interface is hence generated. This thermocapillary stress will drive convective motion in the liquid phase. Fluid moves from low surface tension (high temperature) to high surface tension (low temperature) as observed experimentally (Sefiane and Steinchen 2002). A thermocapillary convective cell will pump hot liquid from the bulk altering the interfacial temperature profile, which will influence the evaporating rate. This study presents a non-conventional Marangoni flow because it is arising from evaporation. Furthermore, thermal energy is removed from the liquid resulting in local changes in the temperature and thus in surface tension. This mechanism has been investigated and discussed under other conditions in many recent works. Such evaporative-driven Marangoni flows lead to the formation of coffee rings from drying drops (Deegan, 1998). These flows also have been proposed as a way to elongate DNA chains for subsequent sequencing analysis (Hu and Larson, 2002) and to enhance heat transfer from menisci in inclined capillary tubes. The present work analyses the necessary conditions allowing the appearance of convective motion and its interaction with energy exchange at the L/V interface.

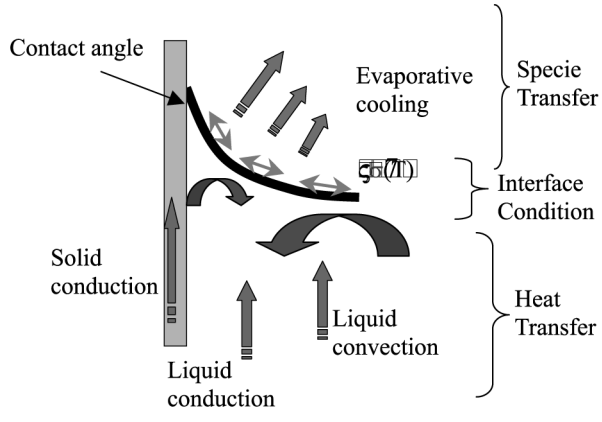

Figure 2.
Heat and mass transfer mechanisms for an evaporating meniscus

Numerical approach

Computational method

The considered meniscus is shown in Figure 2. The configuration involves liquid and vapour phases separated by a L/V interface. In order to avoid the roughness of the tube and the contact angle effect a planar interface is considered to focus on the main interaction between the thermal conditions on the interface and the convection appearing in the liquid phase. An axisymmetric domain is considered for numerical simulation. It consists of a rectangular domain of length L and radius R (Figure 3(a)). The solid wall is maintained at temperature T_0. On the free surface a permanent heat flux is imposed, $Q(r) = Q_0\ q(r)$, where $q(r)$ is a dimensionless function of the axial coordinate r and Q_0 the constant flux case considered as reference heat flux used for the dimensionless temperature. The mass flux across the interface is not considered explicitly and the evaporation is modeled by the heat flux. Concerning the effect of mass flux (interface displacement) we model it via moving reference represented by a Peclet number. For low Pe number we find no significant effect.

Constant, polynomial and Gaussian $q(r)$ distributions (Figure 4) are used to model different evaporation rates at the free surface. The different concentrated

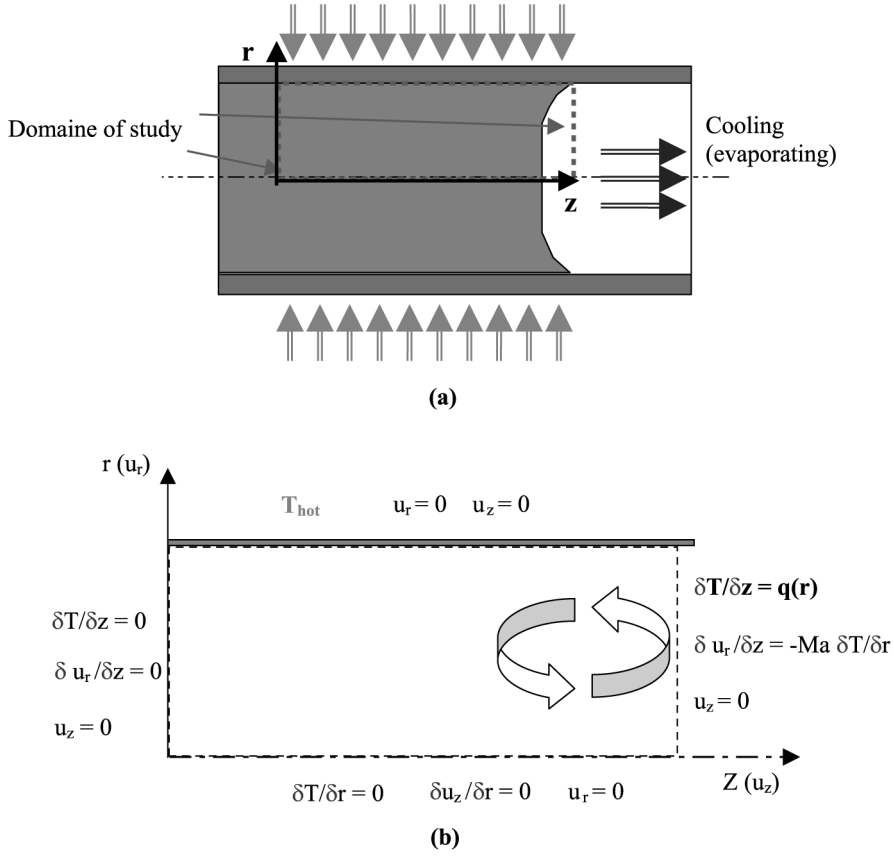

Figure 3.
Schematical global problem (a) and the considered domain for computation (b)

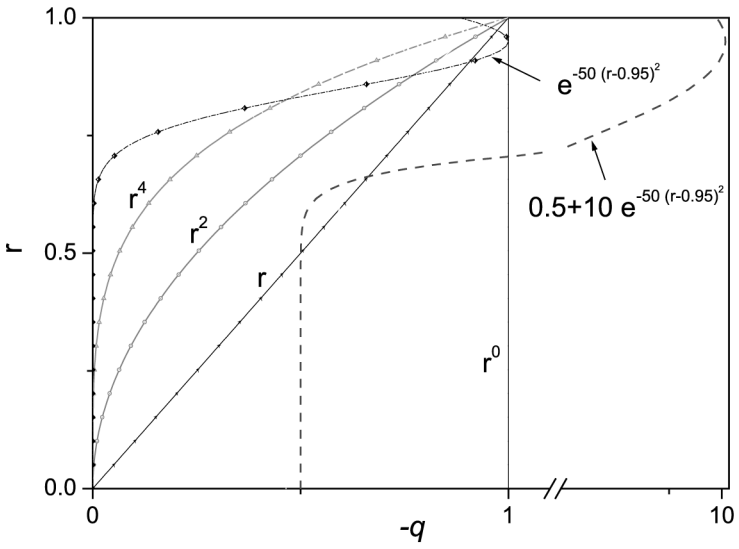

Figure 4.
Various heat flux profile imposed on the L/V interface

profiles allow us to cover evaporation from the isothermal fluid, for the purely conductive case and correlate the interface concentrating effect with the possible superheating effect. We underline that the main goal is the identification of the necessary condition for amplifying the Marangoni convection in order to enhance the evaporation.

The flow is assumed incompressible and laminar for Newtonian fluid. Physical properties (density ρ, dynamic viscosity μ, thermal diffusivity α) are assumed constant and the surface tension σ decreases linearly with the temperature ($\gamma = \partial\sigma/\partial T < 0$).

Using R, α/R^2, $\rho\alpha^2/R^2$ and $Q_0 R/\lambda$, respectively, as the scale factor for the length, time, pressure and temperature, it is possible to write the Boussinesq equation in non-dimensional form as:

$$\nabla \cdot u = 0 \tag{1}$$

$$\frac{\mathrm{d}u_r}{\mathrm{d}t} = -\frac{\partial p}{\partial r} + \mathrm{Pr}\left[\Delta u_r - \frac{u_r}{r^2}\right] \tag{2}$$

$$\frac{\mathrm{d}u_z}{\mathrm{d}t} = -\frac{\partial p}{\partial z} + \mathrm{Pr}\Delta u_z \tag{3}$$

$$\frac{\mathrm{d}T}{\mathrm{d}t} = \Delta T \tag{4}$$

where

$$\frac{\mathrm{d}}{\mathrm{d}t} = \frac{\partial}{\partial t} + u\nabla \text{ and } \Delta = \frac{\partial}{r\,\partial r}\left(r\frac{\partial}{\partial r}\right) + \frac{\partial}{\partial z^2}$$

The dimensionless boundary conditions for the investigated problem are summarised below (shown in Figure 3(b)):

At the symmetry axis $r = 0$,

$$\frac{\partial u_z}{\partial r}(0,z) = \frac{\partial T}{\partial r}(0,z) = 0 \text{ and } u_r(0,z) = 0 \tag{5a}$$

At the solid wall $r = 1$,

$$T(1,z) = 1 \text{ and } u(1,z) = 0 \tag{5b}$$

Imposed heat flux and velocity at the L/V interface:

$$\frac{\partial T}{\partial z}(r,A) = q(r), \quad u_z(r,A) = 0 \quad \text{and} \quad \frac{\partial u_r}{\partial z}(r,A) = -\mathrm{Ma}\frac{\partial T}{\partial r}(r,A) \tag{5c}$$

Far from the L/V interface:

$$\frac{\partial T}{\partial z}(r,0) = 0, \quad u_z(r,0) = 0 \quad \text{and} \quad \frac{\partial u_r}{\partial z}(r,0) = 0 \tag{5d}$$

The dimensionless parameters introduced in equations (1)-(5) are the Prandtl number, $\mathrm{Pr} = \nu/\alpha$ and the Marangoni number $\mathrm{Ma} = -(\partial\sigma/\partial T)\,\Delta T\ R/\mu\alpha$.

The problem is solved in the dimensionless domain $[0,1] \times [0,A]$ ($A = L/R$ is the aspect ratio). In this work, the considered liquid (water, ethanol, etc.) corresponds to $\mathrm{Pr} = 10$ and high aspect ratios are tested to simulate a long tube. The ratio $A = 5$ is found to be sufficient, for a range of Ma, slope and shape of the axial cooling.

A control volume approach (Pantakar, 1980), showing good ability to describe heat and mass transfers for stiff fluid mechanics problems (Raspo and El-Ganaovi, 2002) is used to discretise the governing equations (1)-(4) associated with the boundary conditions (5a)-(5d). The resulting algebraic system is solved using an ADI method coupled to a block correction. The pressure-velocity interlinking is solved using the SIMPLE algorithm. The advection-diffusion terms are approximated using a second-order centred scheme.

Computational details

General validation of the code was undertaken by comparison to the spectral method results of Kasperski and Labrosse (2000); for details see Bennacer *et al.* (2002).

A mesh sensitivity analysis was undertaken and the results are summarised in Table I. Very fine grids near the boundaries are adopted. This refinement is necessary to resolve narrow singularities flow. The relative difference between predictions using

	Nr × Nz	81 × 41	101 × 41	121 × 41	161 × 61	191 × 91	241 × 121
On the free surface	$T_{\min}$	0.910	0.910	0.9121	0.9123	0.9127	*0.913*
	Per cent	0.3[a]	0.3	< 0.2	< 0.1	< 0.1	
$\mathrm{Ma} = 10^2\ Q = r^4$	$u_{r_{\min}}$	− 2.72	2.84	2.90	2.96	2.89	*2.89*
	Percent	6	2	0.5	1	< 0.1	

Note: [a]Deviation between the results (relative to the 241 × 121 case)

Table I. Effect of the mesh refinement on the minimum of T and u on the free surface ($A = 5$, $\mathrm{Ma} = 10^2$ and $\mathrm{Pr} = 10$ for polynomial case)

a 81×41 mesh and the reference grid (241×121) was less than 6.0 per cent for the minimum T and u_r – velocity component on the free surface. The relative difference using a 121×41 is less than 0.5 per cent. A minimum of non-uniform 161×61 grids is used for most computations presented in this paper.

The equations were then solved to ensure conservation of mass, momentum and energy, both globally and locally, to a prescribed tolerance (typically 10^{-6}).

Results and discussion

As mentioned in the "Introduction" the considered sizes ($R < 100\,\mu$m) in the present study, allow us to neglect the Rayleigh convection. Strong thermocapillary convection was observed to be resulting from evaporation. The orientation of the convective cells is found to be dependent on the heat flux distribution along the meniscus. In fact, the real driving force for convection is the tangential capillary stress at the interface generated by the interfacial temperature gradient. This gradient is itself influenced by the convection in the bulk liquid. Indeed, the thermocapillary convection tends to bring hotter liquid from the bulk toward the interface increasing the temperature at the centre and consequently the strength of the convection. The local evaporation rate is dictated by the local vapour pressure, which is strongly dependent on the local temperature and the vapour diffusion from the interface to the gas bulk. Various heat flux distributions are applied along the meniscus to determine conditions under which thermocapillary convection develops (Figure 4). The applied fluxes consider polynomial, Gaussian and combined profiles. The different applied fluxes do not vary on the same range but we see in the "Results and discussion" sections (Figures 7 and 8) that the obtained difference in results is more a matter of profile shape than of order of magnitude. It is worth mentioning that the saturated exponential profile (exp + constant) is the closest one to the realistic profile observed by Kim and Wayner (1996). The direct numerical simulation allows access to the interfacial temperature (Figure 5). It can be noticed that

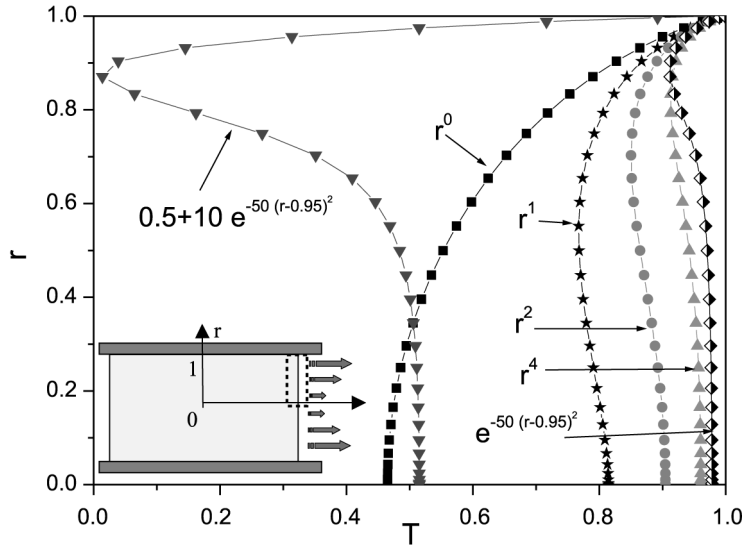

Figure 5.
Interfacial temperatures profiles for the different imposed heat fluxes

the saturated expression induces a temperature profile close to the one observed by Höhmann and Stephan (2002), exhibiting a minimum value near the contact line. The increases of evaporation near the tube ($r = 1$) induce the appearance of colder region with inversion in temperature gradient sign.

Bearing in mind that the radial temperature gradient is the driving force for any convective motion, Figure 6 describes these gradients for the various investigated profiles. As a first observation, the inversion of the temperature gradient occurs for non-linear flux profiles. A polynomial profile induces weak negative radial temperature gradient leading to rotating convective cells from the contact line to the centre in disagreement with experimental observations. Taking saturated exponential shape, the radial temperature gradient presents a minimum value near the contact line with a negative gradient on more than 80 per cent of the interfacial domain. Two regions are distinguished, the first one from the centre to the minimum location where the temperature gradient is supposed to generate a cell rotating from the centre to the contact line. The convective cell developing in the second region (near the corner) rotates in the opposite direction. In the experiment the second cell was not observed, only the main cell rotating from the centre to the contact line has been clearly identified. This can be explained by the fact that friction forces hinder the second convective cell near the wall. This implies that a minimum irregularity in evaporative heat flux will initiate Marangoni convection. An example of obtained temperature and flow field is shown in Figure 7 for Ma = 10. The isotherms (Figure 7(a)) show the non-regular temperature obtained at the L/V interface with the localised cold region (blue colour) near the tube. The heating is assumed via the tube, the evaporation heat extraction is maintained by high temperature gradient near the interface-tube contact and also by the transfer from the bulk via the centre domain (axial direction). The temperature gradient induces two contrarotating cells (Figure 7(b)),

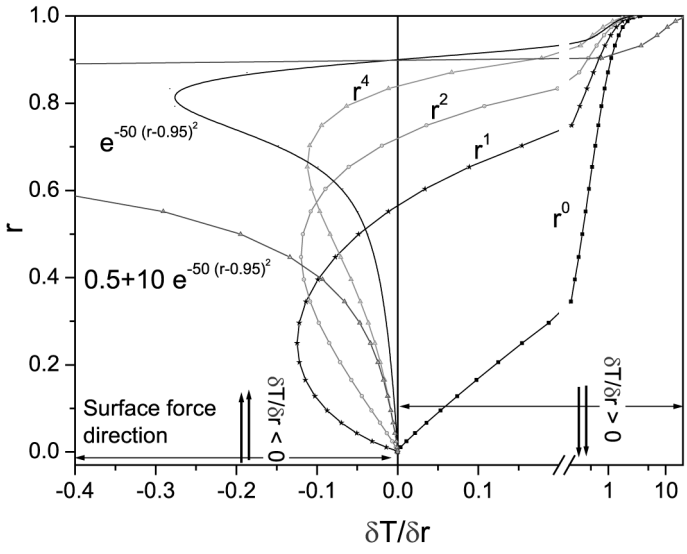

Figure 6.
Temperature gradients distribution for the different applied profiles

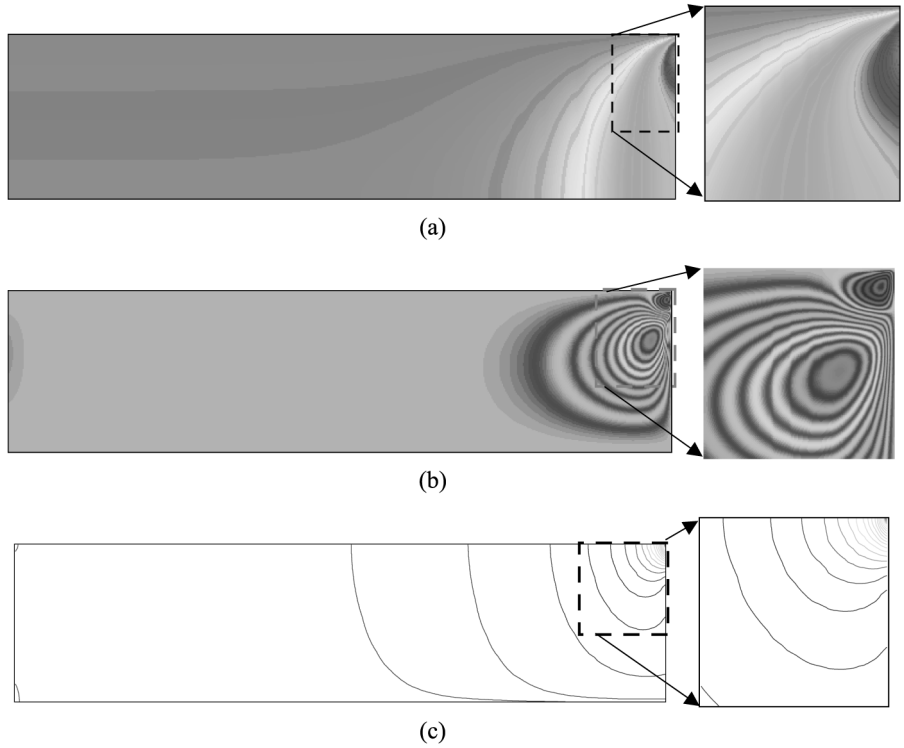

Figure 7.
Isotherms, streamlines and heat lines for Ma = 10 (flux profile of the form: exp + constant)

a major one covering the radial extension and a small weak one. The obtained flow brings hot fluid from the bulk and more energy is convected from the tube toward the interface as illustrated by the heat lines (Figure 7(c)). The presented heat lines allow demonstrating the way followed by the energy and how it follow the resulting flow on the main cell.

Whilst it is experimentally difficult to access the local evaporation rate, the numerical simulation can be an effective tool to describe the controlling parameters. The effect of the convection on the interfacial temperature is investigated by varying the Marangoni number.

Figure 8(a) shows the temperature distribution for various Marangoni numbers. The temperature decreases uniformly near the tube ($r \sim 1$) and is relatively constant on $r = 0 - 1/2$. This shape is similar for various considered Ma. It can be noticed that the minimum value of the interfacial temperature (Figure 8) for different Ma changes little whereas the interfacial temperature at the centre is strongly affected by the Ma variation. The increases of the temperature (in the centre of the tube) with the Marangoni are due to the stronger obtained flow bringing hot fluid from the bulk. The flow increase is illustrated together with the interfacial radial velocity (Figure 8(b)). We can see the sign change corresponding to the two-contrarotating cells explained in the previous section. For higher Ma number the flow shape changes and the main cell is attracted by the tube resulting in a relative non-flow near the axial domain.

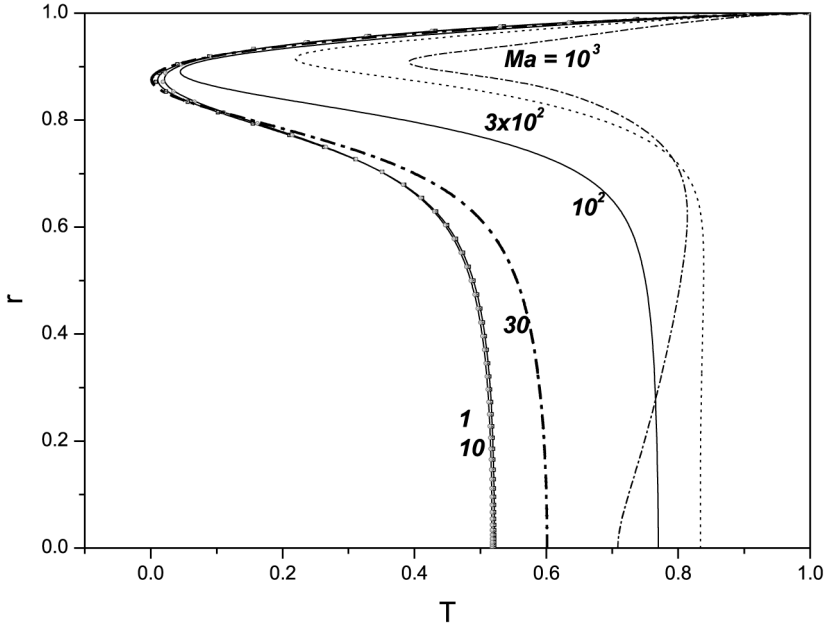

(a)

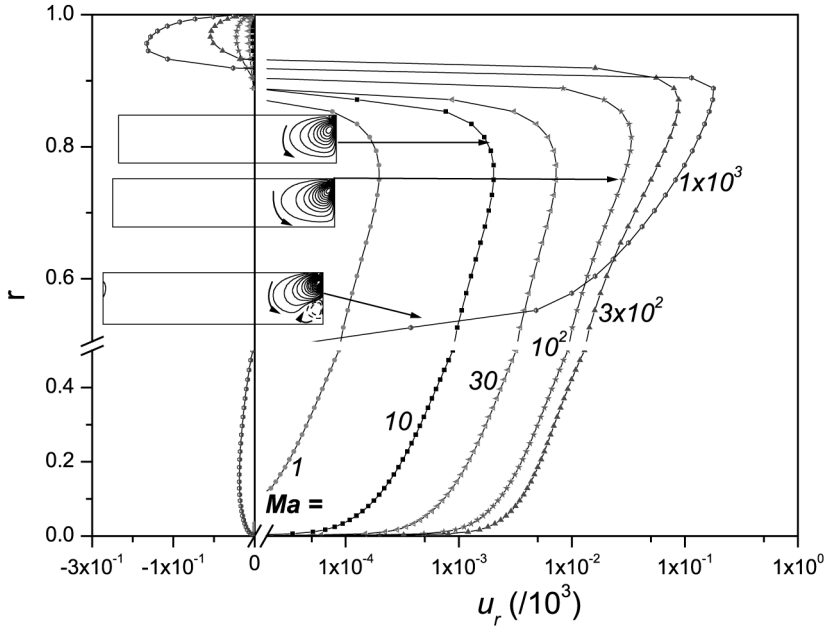

(b)

Figure 8.
Effect of Marangoni number on the interfacial temperature (a) and radial velocity component (b)

Figure 9 represents the maximum of the interfacial radial velocity and the maximum temperature difference on the main cell versus Marangoni number. This temperature difference represents the magnitude of the acting surface forces.

The interesting remark is

- the constant maximum temperature difference in the diffusive problem;
- the increase in the temperature difference with Ma resulting from the increase in flow; the convective motion brings hot fluid to the centre of the interface allowing higher ΔT;
- above a particular Ma value the ΔT decreases with fluid flow coming from the cold region (contact liquid tube point).

The obtained maximum velocity increases with Ma and can be given by the expression $u_{r_{\max}} = 0.11 \times \mathrm{Ma}^{1.24}$. This expression is not valid above the Ma value underlined before. Above this value, we have also the appearance of a new cell in the axis domain. The obtained new cell could be due to the symmetry assumption which physically allows an even number of cells. Loss of symmetry is possible (3D flow) as observed experimentally by Sefiane and Steinchen (2002).

All presented numerical results are obtained for uniform fixed temperature on the tube, which is a valid assumption for tube of high thermal conductivity (low Biot number). In order to check the weight of such an assumption on the obtained result, in the following section, boundary conditions are modified to apply the heat flux on the wall of the capillary.

In terms of fluid flow only the main convective cell is observed (Figure 10). The heating conditions do not permit an inversion of the radial temperature gradient responsible for the observed secondary flow for the previous case of imposed temperature. The isotherms show the irregular temperature value obtained on the tube

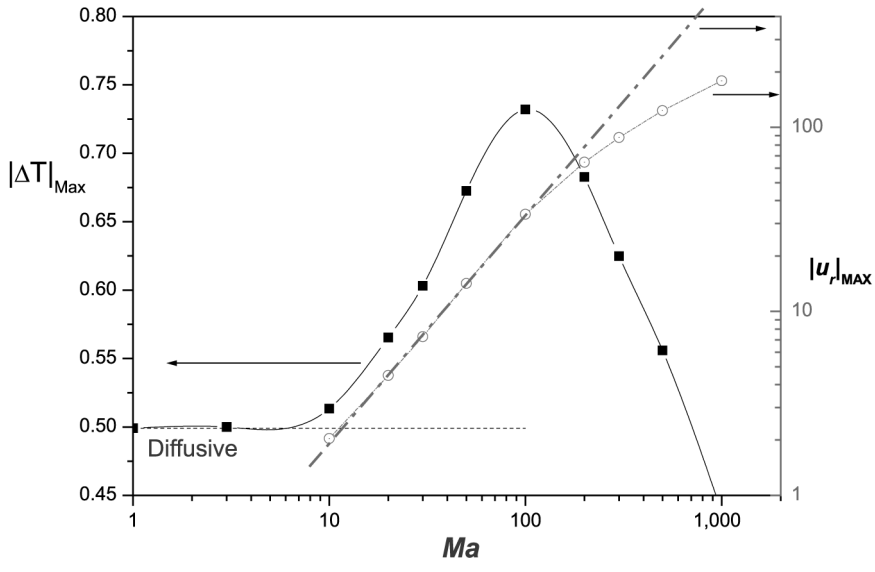

Figure 9.
Maximum temperature difference and maximum velocity versus Marangoni number ($u_{r_{\max}} = 0.11 \times \mathrm{Ma}^{1.24}$)

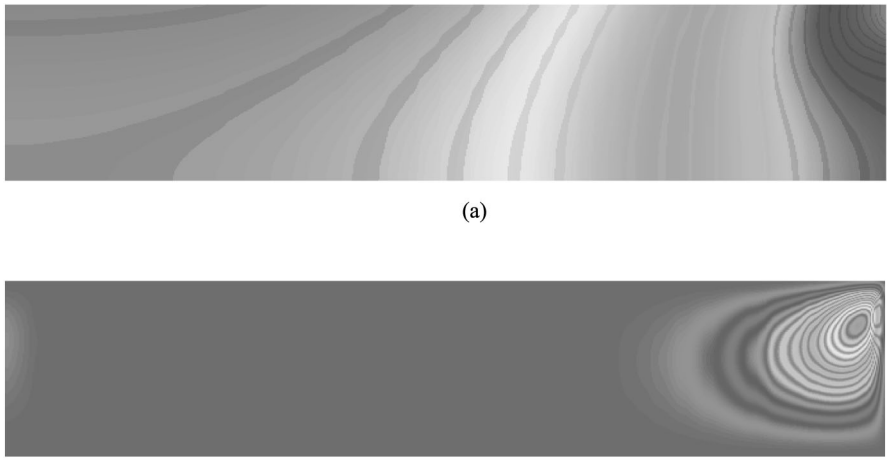

Figure 10.
Isotherms and streamlines for Ma = 10; the tube is submitted to uniform flux

($r = 1$). Physically increasing Ma, allows a better mixing in the liquid and tends to decrease the obtained maximum temperature.

Conclusion

Considered capillary tubes with a small aspect ratio which allows us to neglect the buoyancy convection and to focus on the thermocapillary one. A computational model successfully used for CFD problems involving liquid bridge is extended to capillary tube configurations.

Various heat flux distributions are applied along the meniscus and conditions allowing the development of thermocapillary convection are characterised, the study permits to select a profile close to realistic experimental observations. It is shown that the inversion of the distribution is responsible for the development and the right orientation of the Marangoni cells.

The simulation allows access to the interfacial temperature and to characterise its interaction with Ma convection. Various Marangoni number values are considered to show flow patterns and temperature distribution.

Main fluid flow regimes are identified strating with the diffusive one for low Marangoni number; followed by a convective one exhibiting two behaviours. For moderate Ma, a convective cell occupy the integrity of the domain, flow intensity and temperature difference increases with Ma. For higher Ma, the convective cell is attached to the tube (no flow in the axial domain). Temperature difference decreases with Ma because cold fluid arrives at the interface.

The second regime for critical Ma will be the more interesting one for amplifying evaporation because it allows us to obtain a stronger flow (maximum ΔT) for a lower Ma (critical Marangoni number).

When the tube is submitted to constant heat flux instead of constant temperature, we illustrate the non-existence of the weak secondary cell attached to the corner (L/V interface-tube).

The work continues to analyse the complex interaction between the evaporative mass flux profile and convection developing in the liquid phase to identify optimal operating parameters for application to liquid-vapour phase changes in confined environments.

References

Bennacer, R., Mohamad, A.A. and Leonardi, E. (2002), "Computational analysis of Marangoni effects during floating zone growth under microgravity conditions in heat transfer", *Numerical Heat Transfer, Part A*, Vol. 41, pp. 657-71.

Deegan, R. (1998), "Pattern formation in drying drops", *Physical Review E*, Vol. 61 No. 1, pp. 475-85.

Holm, F. and Goplen, S. (1979), "Heat transfer in the meniscus thin-film transition region", *Journal of Heat Transfer*, Vol. 101, pp. 543-7.

Höhmann, C. and Stephan, P. (2002), "Microscale temperature measurement at an evaporating liquid meniscus", *Experimental Thermal and Fluid Science*, pp. 157-62.

Hu, H. and Larson, R.G. (2002), "Evaporation of a sessile droplet on a substrate", *Journal of Physical Chemistry B*, Vol. 106, pp. 1334-44.

Kasperski, G. and Labrosse, G. (2000), "On the numerical treatment of viscous singularities in wall-confined thermocapillary convection", *Physics of Fluids*, Vol. 12, pp. 2695-7.

Khrustalev, D. and Faghri, A. (1994), "Heat transfer during evaporation and condensation on capillary-grooved structures of heat pipes", Advances in Enhanced Heat Transfer HTD, *ASME*, Vol. 287, pp. 47-59.

Kim, I. and Wayner, P. (1996), "Shape of an evaporating completely wetting extended meniscus", *Journal of Thermophysics and Heat Transfer*, Vol. 10 No. 2, pp. 320-5.

Molenkamp, T. (1998), "Marangoni convection, mass transfer and microgravity", PhD thesis, University of Groningen.

Morris, S. (2001), "Contact angles for evaporating liquids predicted and compared with existing results", *Journal of Fluid Mechanics*, pp. 1-30.

Pantakar, S. (1980), *Numerical Heat Transfer and Fluid Flow*, Hemisphere, New York, NY.

Raspo, I. and El-Ganaoui, M. (2002), *Computations of Instabilities in Complex Fluid Mechanic Problems Using Efficient Finite Volume Methods*, Hermes Penton Sciences.

Sefiane, K. and Steinchen, A. (2002), "On the thermocapillary effects in the evaporation of a meniscus from a capillary tube", *Proceedings of the 12th Int. Heat and Mass Transfer Conf.*, pp. 437-41.